

# The Rate-Controlling Deformation Mechanisms in Superplasticity—A Critical Assessment

A. ARIELI and A. K. MUKHERJEE

The phenomenon of micrograin superplasticity is critically reviewed in the context of the dominant microstructural characteristics, *i.e.*, grain boundary sliding and migration, grain rotation and rearrangement, and dislocation activity. Existing theoretical models consider the accommodation process for grain boundary sliding to be either purely diffusional or due to dislocation motion. The latter can be in the form of individual dislocations or dislocations in the pile-up arrays in the interior of the grains or in grain interfaces. The mechanical properties, *i.e.*, stress, strain-rate, activation energy, threshold stress, and so forth, are compared with the prediction of these models. The extreme sensitivity of the activation energy for superplasticity (which usually equals that for grain boundary diffusion) to alloy or impurity content is emphasized. The very large influence to prior thermal and mechanical history of the specimens on the mechanical data is discussed in the context of alteration of the significant details of grain boundary substructure.

## I. INTRODUCTION

THE phenomenon of micrograin superplasticity in which metals and alloys deform extensively at elevated temperatures under small stresses without risk of rupture has been well documented over the past decade.<sup>1-8</sup> A typical double logarithmic plot of the applied true stress vs the resulting true strain rate at constant test temperature, grain size, and substructure is shown in Figure 1. The plot in Figure 1 can be divided into four regions, *i.e.*: (i) at high stresses a region (Region III) characterized by a slope ( $\equiv$  stress sensitivity,  $n$ )  $\approx 4$  to 5, activation energy for deformation close to that for lattice self-diffusion, the strain rate independent of grain size and contribution of grain boundary sliding (GBS) to total axial creep strain  $\approx 20$  pct; (ii) at intermediate stresses (Region II) there is a second power dependence of strain rate on stress, activation energy for deformation similar to the activation energy for grain boundary self-diffusion, inverse square dependence of strain rate on grain size, and the GBS contribution to the total strain increases to  $\approx 60$  pct; (iii) at low stresses (Region I) the stress sensitivity coefficient is approximately 3 to 4, the activation energy for deformation is, again, close to that for lattice self-diffusion and the GBS's contribution to the axial strain decreases to  $\approx 20$  pct, although the inverse second power dependence of strain rate on grain size remains unchanged; (iv) at still lower stresses than those corresponding to Region I, diffusional creep (either through lattice or along grain boundaries) occurs. In many investigations<sup>9-17</sup> the Region I is absent altogether regardless of whether diffusional creep region was attained or not.

The superplastic materials are attractive mainly for the large ductilities they exhibit at intermediate strain rates (*i.e.*, those corresponding to Region II). Therefore, our understanding of the rate-controlling mechanisms for super-

A. ARIELI, formerly with the Division of Materials Science and Engineering, Department of Mechanical Engineering, University of California, Davis, CA 95616, is now with Northrop Corporation, Aircraft Division, Hawthorne, CA 90250. A. K. MUKHERJEE is with the Division of Materials Science and Engineering, Department of Mechanical Engineering, University of California, Davis, CA 95616.

This paper is based on a presentation made at the symposium "On the Mechanical, Microstructural and Fracture Processes in Superplasticity" held at the annual meeting of the AIME in Pittsburgh, PA on October 7, 1980 under the sponsorship of the Flow and Fracture Activity of the Materials Science Division of ASM.

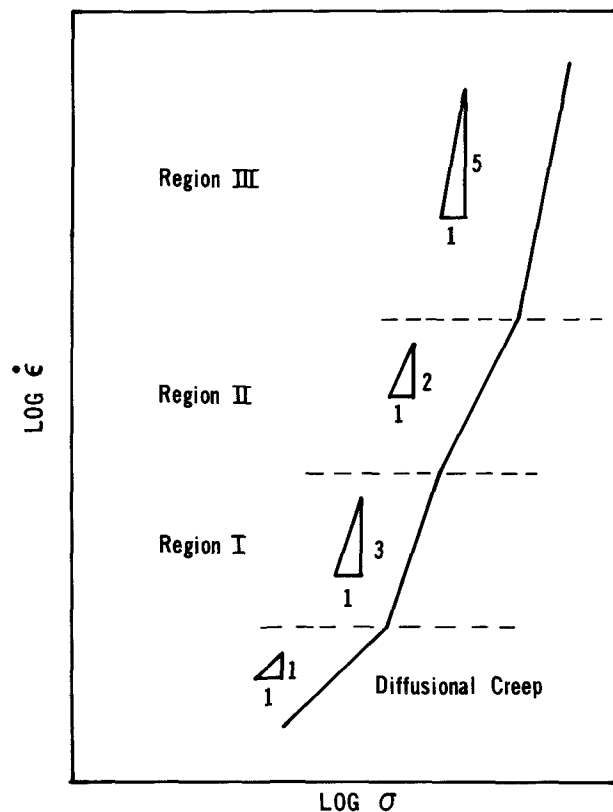


Fig. 1—Schematic stress-strain rate behavior for superplastic materials.

plastic deformation in Region II is important not only for its intrinsic scientific value but also because of its significance in modeling the processing parameters for forming operations. Furthermore, most of the metals and alloys known to behave superplastically in certain ranges of strain rate, grain size, and temperature were not originally developed to maximize superplastic properties. In order to develop new superplastic alloys with optimum properties, a sound theoretical understanding of the dependence of strain rate on flow stress, grain size, temperature, and substructure is imperative.

It is the purpose of this paper to compare the models proposed in literature for the rate-controlling mechanisms in Region II of superplasticity and discuss them in the context

of more recent experimental data on mechanical properties and microstructure from the literature.

## II. DEFORMATION MECHANISMS

### A. Dominant, Rate-Controlling, and Operative Deformation Mechanisms

Micrograin superplasticity is observed at temperatures above about one-half of the melting temperature and at stresses where most metals and alloys deform by diffusion-controlled creep.<sup>18</sup> There are several diffusion-controlled deformation mechanisms<sup>18</sup> which have now been identified. Although in parallel processes many deformation mechanisms can be operative at any one time, usually one causes the fastest deformation rate and therefore becomes rate-controlling and dominant\* over special ranges of stress,

\*In this paper, the dominant deformation mechanism is the mechanism that makes the largest single contribution to the total strain.

grain size, and temperature. A majority of experimental data suggest that GBS is the dominant mechanism in the superplastic deformation process. What makes micrograin superplasticity special in the context of diffusion-controlled deformation mechanisms is that the dominant mechanism (e.g., GBS) cannot also be rate-controlling at the same time. GBS cannot occur continuously on all interfaces (grain or phase-boundaries) without some accommodation in the interface or within the grains themselves.

### B. Accommodation for GBS

In polycrystalline materials two grains cannot slide past each other without impinging on a third grain. Unless the grains deform by intracrystalline slip, they must rearrange themselves in such a way that a pair of grains moves between two others that separate longitudinally, thus lengthening the specimen. The sequence can repeat at many places until the specimen is only a few grains wide, which produces the large extensions that typify superplasticity. In a realistic model for grain rearrangement the grain movement is 3-dimensional; grains move out of their original planes in the specimen and fill voids opened in other parallel planes and increase the surface area of the specimen. The movement of the grains within the specimen occurs by GBS, and in order to rearrange themselves the grains suffer shape change. However, because the various interfaces present in specimens have different properties, the rates of sliding at these interfaces are different and grains rotate during deformation.<sup>19</sup> Thus, a grain which elongated longitudinally previously following rotation will elongate in other directions and, hence, no marked departure from the equiaxed shape of the grain is observed. Hence, upon application of stress, the specimen changes shape which is brought about by grain rearrangement. The latter, in turn, is due to GBS (and grain rotation). Therefore, the specific process that accommodates the GBS will be the rate controlling step.

Another problem with GBS's accommodation is the attainment of steady-state. If steady-state is to be achieved, the interface structure must remain constant during deformation. With a few exceptions (which do not apply to superplasticity) constant interface structure can be achieved only if sliding is accompanied by migration.<sup>20</sup>

All the deformation mechanisms presented in this paper are based (explicitly or implicitly) on the microscopic aspects described above.

## III. DESCRIPTION OF THE PROPOSED MODELS FOR THE RATE-CONTROLLING MECHANISM IN REGION II OF SUPERPLASTICITY

The accommodation mechanisms for GBS proposed in the literature can be divided into two groups, namely, diffusional accommodation<sup>21</sup> and accommodation due to dislocation motion. The dislocation motion accommodation mechanisms can be further grouped into accommodation process due to dislocation pile-ups (either inside the grains<sup>22,23,24</sup> or in the interfaces<sup>25,26,27</sup>) and that due motion of individual dislocations.<sup>28,29,30</sup>

### A. Diffusional Accommodation

#### Ashby and Verall Model<sup>21</sup>

These authors put forward a model which explains superplasticity as a transition region between the diffusion-accommodated flow, operative at low strain rates, and diffusion-controlled dislocation climb at high strain rates.

At low strain rates where diffusion-accommodated flow accounts for more than 99 pct of the total strain rate, the specimen elongation is accomplished by grain rearrangement which in turn takes place by grain boundary sliding. In order for grains to maintain compatibility during the deformation process, they must suffer a transient but complex shape change or accommodation strain. This accommodation is accomplished by diffusional transport. Due to transient increase in the grain boundary area during grain rearrangement process, the deformation is limited at very low strain rates by a threshold stress. Characteristic of this model is the fact that units of four grains must deform cooperatively in order to achieve a unit strain of 0.55 and, at the same time, maintain compatibility across grain boundaries.

At high strain rates, where dislocation creep accounts for more than 99 pct of the total strain rate, the specimen elongation is achieved by the change of shape of the individual grains. At intermediate strain rates these two mechanisms superimpose on each other, each one contributing more than one pct to the total strain rate. The microstructural and topological features of the plastic flow at these strain rates will be those characteristic of the two mechanisms. Since these two processes are independent and take place simultaneously, the total strain rate,  $\dot{\epsilon}_{tot}$ , will be the sum of the strain rates contributed by each process, i.e.,

$$\dot{\epsilon}_{tot} = \dot{\epsilon}_{diff. acc} + \dot{\epsilon}_{disloc. creep} \quad [1]$$

where

$$\dot{\epsilon}_{diff. acc} = 100 \frac{\Omega}{kT d^2} \left\{ \sigma - \frac{0.72 \Gamma}{d} \right\} D_1 \left\{ 1 + \frac{3.3\delta D_b}{d D_1} \right\} \quad [2]$$

and

$$\dot{\epsilon}_{disloc. creep} = A \frac{D_1 G b}{kT} \left\{ \frac{\sigma}{G} \right\}^n \quad [3]$$

The values taken by parameters  $A$  and  $n$  in Eq. [3] will depend upon the specific dislocation creep mechanism found operative at high strain rates for the material under investigation.<sup>31,32</sup>

When Eq. [1] is expressed in an emirical form as

$$\sigma = \text{const.} \cdot \dot{\epsilon}^m_{\text{tot}} d^p \exp\left\{\frac{Q}{RT}\right\} \quad [4]$$

the model predicts that  $m$  is a strong function of strain rate with a maximum, at a strain rate close to that corresponding to diffusional creep, approaching unity but never quite reaching it. Furthermore,  $m$  is predicted to be dependent on temperature and grain size. The grain size dependence coefficient,  $p$ , will vary between 0 and 3 depending upon the strain rate and temperature. The model also predicts that the activation energy for superplastic flow will be dependent upon temperature and stress, varying between the value of the activation energy for grain-boundary diffusion and that for lattice self-diffusion.

## B. Dislocation Pile-Up Accommodation

### 1. Pile-ups within the Grains

#### Ball and Hutchison<sup>22</sup> and Mukherjee<sup>23</sup> Models

Ball and Hutchison<sup>22</sup> proposed that groups of grains slide as a unit until unfavorably oriented grains obstruct the process. The resultant stress concentration is then relieved by dislocation motion in the blocking grains. These dislocations pile up against the opposite grain-boundary until the back stress prevents further activation of the source and stops sliding. The leading dislocation in the pile-up can thus climb into and along the grain-boundaries to annihilation sites.

Mukherjee<sup>23</sup> has proposed a modification of the above model in which grains slide individually rather than in groups. Dislocations are generated by ledges and protrusions in the grain-boundaries, traverse the grain, and are again held up in pile-ups at grain-boundaries. The rate of sliding is then controlled by the climb rate of the lead dislocation into annihilation sites located at grain-boundaries.

The models lead to the following rate equations

$$\frac{\dot{\epsilon}kT}{D_bGb} \approx 200 \left(\frac{b}{d}\right)^2 \left(\frac{\sigma}{G}\right)^2 \quad [5]$$

for Ball-Hutchison<sup>22</sup> model, and

$$\frac{\dot{\epsilon}kT}{D_bGb} \approx 2 \left(\frac{b}{d}\right)^2 \left(\frac{\sigma}{G}\right)^2 \quad [6]$$

for Mukherjee<sup>23</sup> model.

Eqs. [5] and [6] are almost identical, differing only by the value taken by the substructure related parameter which takes the value of 200 and 2 in References 22 and 23, respectively. It should be mentioned that, whereas the value of this parameter was calculated theoretically, from the dislocation climb theory in Mukherjee's model, the value of 200 in Eq. [5] was obtained by fitting the rate-equation to the experimental data.

### 2. Pile-ups in the Interfaces (Grain-and/or Phase-Boundaries)

#### (a) Mukherjee<sup>24</sup> Model

Mukherjee<sup>24</sup> proposed a modified version of his original

model<sup>23</sup> where the grain-boundary sliding is rate-controlled by dislocation motion not across the grains, but by motion of the dislocations in the grain-boundary by a climb-glide process. The compatibility between the adjacent grains is achieved by diffusion-controlled climb of lattice dislocations along the grain boundaries, thus allowing for the repeated accommodation that is necessary for the operation of grain-boundary sliding as a unit process. The combination of grain-boundary sliding and dislocation climb leads to grain rearrangement and accounts for the absence of grain elongation during superplastic flow.

The rate equation

$$\frac{\dot{\epsilon}kT}{D_bGb} \approx (75-150) \left(\frac{b}{d}\right)^2 \left(\frac{\sigma}{G}\right)^2 \quad [7]$$

is identical to Eqs. [5] and [6] but with the substructure related parameter taking now values between 75 and 150, with an average value of 100.

#### (b) Gifkins<sup>25,26</sup> Model

In this model, sliding is considered to take place by the motion of grain-boundary dislocations that pile up at triple points. The resulting stress concentration is relaxed by dissociation of the leading grain-boundary dislocation capable of moving in the two other boundaries making up the triple point, and/or into lattice dislocations which accommodate sliding. These new dislocations then climb or glide in or near these two boundaries until they meet each other. Then they may annihilate or combine with them to form different grain-boundary dislocations. This complete sequence of events will produce grain rotation and rearrangement in agreement with microstructural studies. The rate equation according to this model is identical to Eqs. [5] to [7] except that the substructure related parameter is 64. The physical basis of this model, however, puts emphasis on the role played by grain-boundary dislocations.

An important feature of this model is that it does not require that the compatibility between adjacent grains be maintained at all stages of the deformation. Instead, as proposed by Hazzeldine and Newbury,<sup>33</sup> gaps (voids) are opened at interfaces to be filled up by grains sliding from adjacent planes in the specimen.

#### (c) Gittus<sup>27</sup> Model

A theory for superplastic deformation in two-phase materials has been proposed by Gittus.<sup>27</sup> It is postulated the grain-boundary dislocations, piled up in interphase-boundaries (IPB), climb away into adjacent disordered segments of the IPB. Sources in the IPB operate and introduce new dislocations to replace those that have climbed away from the head of the pile-up. Sliding occurs at the IPB's as the dislocations in the pile-up glide toward the head of the pile-up. The flow of matter to the dislocations as they climb the disordered regions of grain boundary permits the changes in shape that are needed to preserve continuity of the boundaries during deformation. The model incorporates a threshold stress which is identified with the pinning interaction between interphase boundary superdislocations and boundary ledges of dislocation character. The activation energy is theoretically that for IPB diffusion. According to this model the superplastic strain-rate is given by:

$$\frac{\dot{\epsilon}kT}{D_{\text{IPB}}Gb} = 53.4 \left(\frac{b}{d}\right)^2 \left\{\frac{(\sigma - \sigma_0)}{G}\right\}^2 \quad [8]$$

### C. Accommodation by the Motion of the Individual Dislocations

#### (1) Hayden, Floreen, and Goodell<sup>28</sup> Model

This model predicts that grain-boundary sliding is rate-controlled by the rate of intergranular dislocation creep. Dislocations are nucleated at grain-boundary triple-points and ledges, traverse the grain by glide and climb and then climb, individually without forming pile-ups, into opposite grain boundaries where they are annihilated.

The model postulates that at a critical temperature,  $T_c$ , there will be a transition in the diffusion mechanism from pipe (at  $T < T_c$ ) to lattice diffusion ( $T > T_c$ ). At  $T_c$  the climb velocities controlled by these two diffusion mechanisms will be equal. Furthermore, the model suggests that the rate of sliding is related to the rate of intragranular dislocation creep by a geometrical constant, which will be independent of material and temperature, and that the ratio of sliding rate to dislocation creep rate will vary inversely with the grain size.

Depending upon whether or not the sliding rate, as determined by the dislocation climb rate, will be less or equal to the theoretical maximum possible sliding rate, as determined by grain-boundary viscosity, and on the deformation temperature, *i. e.*,  $T < T_c$  or  $T > T_c$ , the authors<sup>28</sup> predict four different rate equations.

Basically, for the superplastic region, the model will predict

$$\frac{\dot{\epsilon}kT}{D_p Gb} \propto \left(\frac{b}{d}\right)^3 \left(\frac{\sigma}{G}\right)^2 \quad [9]$$

for  $T < T_c$ , and

$$\frac{\dot{\epsilon}kT}{D_l Gb} \propto \left(\frac{b}{d}\right)^2 \left(\frac{\sigma}{G}\right)^2 \quad [10]$$

for  $T > T_c$ .

#### (2) Spingarn and Nix<sup>29</sup> Model

This model considers the deformation to occur by intragranular slip along slip bands which are blocked by grain boundaries, the strain at the boundary being accommodated by diffusional flow in the boundaries resulting in a steady-state creep process. The slip band spacing varies with the strain rate, *i. e.*, decreases as the strain rate is increased. In the limit of very small stresses the slip band spacing is equal to grain size,  $d$ , and the rate equation is given by

$$\frac{\dot{\epsilon}kT}{D_b Gb} = 100 \left(\frac{b}{d}\right)^3 \left(\frac{\sigma}{G}\right) \quad [11]$$

where we have taken  $\Omega = b^3$  and  $\delta = 2b$ . Eq. [11] is essentially identical to the pure diffusional creep by the Coble mechanism.<sup>34</sup>

At very large stresses, the slip band spacing is taken to be equal to the subgrain size, and the rate equation is given by

$$\frac{\dot{\epsilon}kT}{D_b Gb} = (\text{const.}) \left(\frac{d}{b}\right) \left(\frac{\sigma}{G}\right)^5 \quad [12]$$

The authors<sup>29</sup> suggest that the transition zone (which spans more than an order of magnitude in stress) from  $n = 1$  (Eq. [11]) to  $n = 5$  (Eq. [12]) behavior coincides with the superplastic range. No specific rate equation is given for the superplastic region, although the total strain rate in this region must be different from the simple sum of

the rates given by Eqs. [11] and [12], since the slip band spacing varies with strain rate.

According to this model, not only  $n$  varies from 1 to 5 but also the strain rate dependence on grain size coefficient will vary between  $-3$  and  $+1$ . The activation energy for deformation will be that for grain-boundary diffusion.

#### (3) Arieli, Mukherjee<sup>30</sup> Model

In this model, the individual lattice dislocations in a narrow region near the interfaces will climb directly into and/or along the interfaces, being annihilated into the interfaces. During the climb process the dislocations multiply by a Bardeen-Herring<sup>35</sup> mechanism, thus making this process self-regenerative. Due to the close proximity to the interfaces, the climb of the individual dislocations will be controlled by the grain-boundary diffusion. At high stresses more dislocations will arrive at the interfaces from the grain interior, the critical step then being the overcoming by these dislocations, of the obstacles to their motion inside the grains, by glide and climb process controlled by lattice diffusion.

The model predicts a superplastic strain rate given by

$$\frac{\dot{\epsilon}kT}{D_b Gb} = \left[ \frac{4\pi\omega}{hZ^2 \tan \frac{\theta}{2}} \right] \left(\frac{b}{d}\right)^2 \left(\frac{\sigma}{G}\right)^2 \quad [13]$$

The model predicts that the substructure related parameter will not be a geometrical constant, but will vary with both interface structure (through  $h$  and  $\theta$ ) and the structure of the narrow zone near the interface (through  $\omega$  and  $Z$ ). Also, this model incorporates the effect of grain-boundary migration on the superplastic strain rate.

## IV. COMPARISON WITH EXPERIMENT

### A. Microstructural

#### (1) Grain Rotation and Rearrangement

All the models presented in the previous section can predict the observed grain rotation and rearrangement during superplastic flow. Beere<sup>19,36</sup> has shown that differences in the resistance to sliding of various interfaces present in superplastic materials will create significant friction stresses at the sliding interfaces, thus leading to grain rotation. Therefore, any model assuming the sliding at the interfaces to be dominant (and all the above models do) will predict, explicitly or implicitly, grain rotation. The only condition will be the existence of more than one type of interface, in other words, the existence of at least two phases. Discounting the pure metals where enhanced ductility was observed,<sup>37,38,39</sup> and quasi single phase alloy<sup>40,41</sup> with precipitates at grain boundaries, the vast majority of materials exhibiting superplasticity are multiphase alloys.

During superplastic flow, a tensile specimen will increase its surface area and reduce its thickness. In the absence of recrystallization the grains maintain their identity and, in order to accommodate the change in the physical shape of the specimen, they will rearrange themselves by moving out of their original plane in the specimen. Such a three-dimensional grain rearrangement takes place by sliding at

interfaces, and as long as transient gaps (voids) are allowed to occur at the interfaces no additional accommodation is necessary. All the models discussed in this paper can predict such three-dimensional grain rearrangements; however, only two models<sup>25,26,30</sup> explicitly include such a process. Although the Ashby-Verall<sup>21</sup> model might be visualized to incorporate such 3-D grain rearrangements, their rate equation will have to be modified since it specifically incorporates the transient grain shape change required to maintain compatibility during 2-D grain rearrangements.

## (2) Grain Shape

One of the most striking features of superplasticity is the fact that grains maintain their essentially equiaxed shape even after specimen elongations of hundreds and thousands pct. Here again, the assumption that interface sliding is the dominant deformation mode can explain the experimental observations. Regardless of the specific accommodation mechanism (diffusional or dislocation motion) for sliding, grain rotation and rearrangement will continuously bring new slip planes or boundary segments in the most favorable orientation with respect to the major deformation axis and, hence, there will be no marked departure from the equiaxed grain shape in any specific direction.

## (3) Dislocation Activity

Detailed T. E. M. and texture investigations have proved beyond any doubt that significant dislocation activity occurs during superplastic flow. These observations were recently reviewed<sup>7,8</sup> in some detail and will not be repeated here.

All the models<sup>21-24,28,29</sup> involving intragranular slip predict the TEM and texture observations. The model based on the accommodation of sliding by local climb of individual dislocations<sup>30</sup> predicts gross intragranular activity only in the grains which fill the gaps opened during 3-D grain arrangements. Since the superplastic materials usually have quite uniform grain size and shape, the grains moving out of their original planes in the material had to be "extruded" in order to accommodate the size and the shape of the gap (void) they fill. Such grain "extrusion" cannot be confined to a narrow region near the boundaries and, hence, intragranular slip occurs. Since, as shown by Hazzeldine and Newbury,<sup>33</sup> at  $\epsilon = 0.8$  and  $\epsilon = 1.39$ , one third and one half, respectively, of the grains have moved out of their original plane in the material, considerable intragranular dislocation activity can be detected by TEM and/or texture studies following superplastic flow. Although it is not mentioned in the original models,<sup>25,26,27</sup> the same explanation holds for the models involving accommodation by grain-boundary dislocation motion.

## (4) Interface Sliding and Migration

Only limited work was performed to distinguish among the sliding interfaces, *i. e.*,  $\alpha$ - $\alpha$ ,  $\beta$ - $\beta$ ,  $\alpha$ - $\beta$ , and so forth,<sup>42,43,44</sup> or to investigate the effect of the orientation of the sliding interface relative to the applied stress.<sup>45</sup> The amount and the rate of sliding varies with the type of interface and seems to be directly related to the differences in the grain-boundary diffusivities of the various interfaces,<sup>44</sup> *i. e.*, the faster the grain-boundary diffusivity for a given interface, the larger the amount of sliding for constant  $\dot{\epsilon}$  and  $\epsilon$ . This observation seems to support those models<sup>22-26,29,30</sup> which predict that grain-boundary diffusion will control the deformation rate. Valiev and Kaybishev<sup>45</sup> found that in the

superplastic regime the amount of sliding at the boundaries making angles of 45 deg and 90 deg to the tensile axis was, respectively, 50 pct and 33 pct larger than that taking place at the boundaries lying parallel to the tensile axis. These results seem to indicate circumstantial support for models involving accommodation by dislocation motion.

As was mentioned briefly in Section II, grain-boundary migration can play an important role in the superplastic flow phenomenon. Not only was grain-boundary migration found to accompany grain-boundary sliding in coarse grained materials,<sup>46,47</sup> but also its occurrence is required in order to maintain the interface structure unchanged during sliding.<sup>20</sup> Only one model<sup>30</sup> incorporates the effect of grain-boundary migration on the superplastic strain rate. The overlooking of the effects of grain-boundary migration in models based on interface sliding as the dominant deformation mechanism has important implications. An unstable interface structure during superplastic flow might lead to reduced or increased sliding rates, requiring more or less accommodation than a stable boundary structure and, therefore, leaving open the possibility that other accommodation mechanisms in addition to the one postulated in the models are needed to maintain the externally imposed deformation rates. Operation of such additional accommodation mechanisms within the superplastic range can lead to loss of the superplastic behavior.

## (5) Summary

The major microstructural and topological characteristics of superplasticity related to the grain structure are:

(a) Considerable amounts of grain-boundary sliding and migration take place during superplastic flow. The rate of sliding varies with the type of interface and the orientation of the interface relative to the tensile stress axis.

(b) Grains rotate during deformation, the sense and the amount of rotation depending upon the immediate surroundings (the neighbor grains).

(c) The imposed strain is accommodated by 3-D grain rearrangements.

(d) The essentially equiaxed grain shape is maintained even after hundreds and thousands pct strain.

(e) Substantial dislocation activity takes place during superplastic flow, as evidenced by TEM and texture studies. However, the extent of the dislocation activity varies from grain to grain and the texture is strengthened in certain directions while it is reduced in other directions.

(f) Considerable grain growth takes place concurrently with superplastic flow.

It is shown that, although not all the proposed models explicitly incorporate the above observations, the assumption that grain-boundary sliding is the dominant deformation mechanism in superplasticity leads to their implicit inclusion in those models. Hence, microstructural studies related to the grain structure cannot completely discriminate among the proposed models for the rate-controlling deformation mechanism in superplasticity.

## B. Phenomenological

### (1) Stress-Strain Rate Behavior

The nature of the plot of  $\log \sigma$  vs  $\log \dot{\epsilon}$  in Region II of superplasticity is still open to debate. Although most recent investigations found it to be a straight line,<sup>9-17,22,25,28,40,41,48-50</sup> there are still many published investigations in the literature<sup>3</sup> where a nonlinear  $\log \sigma$ - $\log \dot{\epsilon}$  is reported. The stress-strain

rate behavior is important, especially in the context of a review of the rate-controlling mechanisms in superplasticity. All the models<sup>22-28,30</sup> which contend that superplasticity is a unique mechanism on its own, predict a linear  $\log \sigma$ - $\log \dot{\epsilon}$  relationship. Only those models<sup>21,29</sup> which try to predict a nonlinear  $\log \sigma$ - $\log \dot{\epsilon}$  relation have to resort to a combination of two mechanisms, thus, the superplasticity being inferred as transition between these two mechanisms. There will inevitably be some scatter in plotting experimental data on a log-log plot of stress vs strain rate. However, a re-analysis of more than 20 published investigations<sup>51</sup> indicates that the data in Region II can be fitted to a straight line of constant slope with correlation coefficients better than 0.94. Why, then, have so many workers reported nonlinear  $\log \sigma$ - $\log \dot{\epsilon}$  behavior? The answer seems to lie in the variation of the stress-rate sensitivity coefficient,  $m$ , with strain rate determined from strain rate change tests. The  $m$ -values determined from such tests invariably show a maximum at some optimum strain rate decreasing at both higher or lower strain rates than the optimum one. Hence, one almost anticipates a nonlinear  $\log \sigma$ - $\log \dot{\epsilon}$  plot in order to accommodate this variation in  $m$ -values. The strain rate change test method for determining  $m$  has been discussed in detail<sup>52,3,53</sup> and was shown to lead to some doubtful numerical values for  $m$ . However, very recently the authors<sup>54</sup> have shown that whether or not there is some experimental bias involved due to test methods, the  $m$ -values determined by strain rate change tests cannot always be used to assess unambiguously the deformation mechanism in superplasticity. Basically, in order to evaluate the flow stress dependence on strain rate the following empirical relation is used

$$\sigma = K\dot{\epsilon}^m \quad [14]$$

The strain rate change tests are based on the assumption that  $K$  in Eq. [14] remains constant during the test. If  $K$  varies during the test (*i.e.*, structural changes take place during the test), then the  $m$ -value thus obtained does not indicate the true strain rate sensitivity of the flow stress during steady-state and, hence, cannot be used to identify the specific deformation mechanism. Figures 2(a) and (b) show typical  $\ln \sigma$  vs  $\ln \dot{\epsilon}$  and  $m$  vs  $\ln \dot{\epsilon}$  plots, respectively, for superplastic deformation. Figure 2(c) shows the variation of  $\dot{\epsilon}^m$  with  $\ln \dot{\epsilon}$ . Since the strain rates where superplastic behavior is observed are less than unity and  $m$  increases continuously with the increasing strain rate up to  $\dot{\epsilon}_{opt}$ ,  $\dot{\epsilon}^m$  will decrease continuously as  $\dot{\epsilon}$  increases, a minimum being reached at  $\dot{\epsilon}_{opt}$ . At strain rates higher than  $\dot{\epsilon}_{opt}$ ,  $m$  falls rapidly and  $\dot{\epsilon}^m$  increases. For the results shown in Figure 2(c), according to Eq. [14], at constant  $K$  the flow stress should decrease with increasing strain rate up to  $\dot{\epsilon}_{opt}$  and then increase. However, experiments show that  $\sigma$  increases continuously with increasing  $\dot{\epsilon}$  (Figure 2(a)). Therefore, in order for Eq. [14] to hold,  $K$  should vary with  $\dot{\epsilon}$ . This variation is shown in Figure 2(d). Based on the above arguments, it seems conceivable that  $m$ -values determined from strain rate change tests represent an index of the ability of the material to withstand neck growth,<sup>3</sup> *i.e.*, are related to the mechanics of plastic flow, whereas  $m$ -values determined from the constant slopes of the curves in the  $\log \sigma$ - $\log \dot{\epsilon}$  plots represent the true stress-strain rate relationship, *i.e.*, are related to the mechanism of plastic flow.\*

\*This remark does not apply to the case where the  $m$  value is determined from slope of  $\log \sigma$  vs  $\log \dot{\epsilon}$  plot, but the  $\sigma$  and  $\dot{\epsilon}$  data themselves are gathered from strain rate change tests.

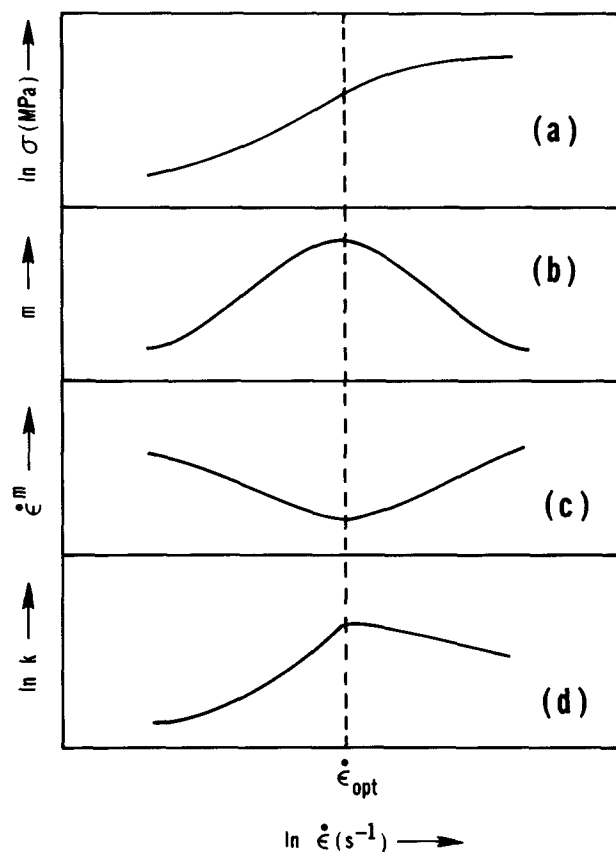


Fig. 2—Schematic plots of  $\ln \sigma$ , (a);  $m$ , (b);  $\dot{\epsilon}^m$ , (c), and  $\ln k$ , (d) vs  $\ln \dot{\epsilon}$ .

Only three of the models<sup>21,27,29</sup> discussed here specifically describe a nonlinear  $\log \sigma$ - $\log \dot{\epsilon}$  behavior. One of them<sup>21</sup> uses the principle of superposition of two mechanisms to account for  $m$  variation with strain rate. Spingarn and Nix<sup>29</sup> implicitly assume the structure to vary with  $\dot{\epsilon}$  and, therefore, no  $\log \sigma$ - $\log \dot{\epsilon}$  plot can be constructed at constant structure. The third model<sup>27</sup> invokes the existence of a threshold stress. The problem of the threshold stress will be considered in the next section.

## (2) Threshold Stress

Two of the models considered here invoke the existence of a threshold stress.<sup>21,27</sup> The existence of a threshold stress for diffusion creep of materials containing grain-boundary particles is now established.<sup>55</sup> In the Ashby-Verall<sup>21</sup> model the groups of four grains increase their boundary area in a transient manner by an amount of  $0.26 d^2$  and, although the energy stored during the transient step is released when the final state is achieved, no energy transfer to another group of grains is possible. The result is a threshold stress given as:

$$\sigma_0 \approx \frac{0.72 \Gamma}{d} \quad [15]$$

Typically, for metals  $\Gamma \sim 10^{-6}$  MN/m and for grain sizes between  $10^{-6}$  m and  $10^{-5}$  m, will give  $7.2 \times 10^{-2}$  MN/m<sup>2</sup>  $< \sigma_0 < 7.2 \times 10^{-1}$  Mn/m<sup>2</sup>.

Another source of a threshold stress in Ashby-Verall<sup>21</sup> model is the interface reaction. If boundaries are perfect sources and sinks for point defects, the interface potential,  $\Delta\mu$ , is equal to zero. If, however, boundaries are not perfect sources and sinks for point defects,  $\Delta\mu$  takes a finite value

and some of the applied stress will be dissipated to drive the interfacial reaction. As pointed out by Ashby and Verall,<sup>21</sup> in the absence of a viscous drag opposing the motion of grain-boundary dislocations  $\Delta\mu$  is a constant and an additional threshold stress

$$\sigma_0' \approx 0.84 \Delta\mu \quad [16]$$

is introduced. The threshold stresses given by Eqs. [15] and [16] are simply additive and result in an effective threshold stress given by

$$\sigma_{0\text{eff}} = \frac{0.72 \Gamma}{d} + 0.84 \Delta\mu \quad [17]$$

The threshold stress proposed by Gittus<sup>27</sup> is due to pinning interaction between interphase boundary superdislocations and boundary-ledges of dislocation character. The estimated threshold stress is

$$\sigma_0 \approx \frac{2E}{bL} \quad [18]$$

Since "the boundary defect is regarded as a flexible line" by Gittus,<sup>27</sup> its energy per unit length can be approximated as

$$E \approx 0.5 G b^2 \quad [19]$$

Combining Eqs. [18] and [19] we obtain

$$\sigma_0 \approx \frac{Gb}{L} \quad [20]$$

Experimental data on the magnitude and the dependence of the threshold stress on grain size and temperature during superplastic flow are extremely scarce. One well characterized result is due to Smith and co-workers<sup>56</sup> who investigated such dependence (Figure 3). The results listed in Table I clearly indicate that the threshold stress calculated from the Ashby-Verall model is too small to account for the experimental ones. Furthermore, the experimental threshold stress varies directly with the grain size and inversely with temperature, whereas the theory predicts an inverse relation between the threshold stress and grain size and no dependence on temperature. If the interface reaction is considered, then the interface potential will vary with both grain size and temperature. This variation is shown in the last column in Table I. A simple threshold stress resulting from interface reaction (Eq. [16]) cannot explain this behavior. A possible explanation is that a viscous drag opposes the motion of dislocations and then  $\Delta\mu$  is a function of stress and grain size<sup>21</sup> given by

$$\Delta\mu = \frac{\dot{\epsilon} \Omega d}{\rho b^2 M} \quad [21]$$

and since<sup>18</sup>

$$\rho = \left( \frac{\sigma}{Gb} \right)^2 \quad [22a]$$

Eq. [21] becomes

$$\Delta\mu = \frac{\dot{\epsilon} \Omega d G^2}{\sigma^2 M} \quad [22b]$$

Eq. [22b] indicates that at constant  $\dot{\epsilon}$  and  $d$ ,  $\Delta\mu$  will increase as the temperature increases (through the factor

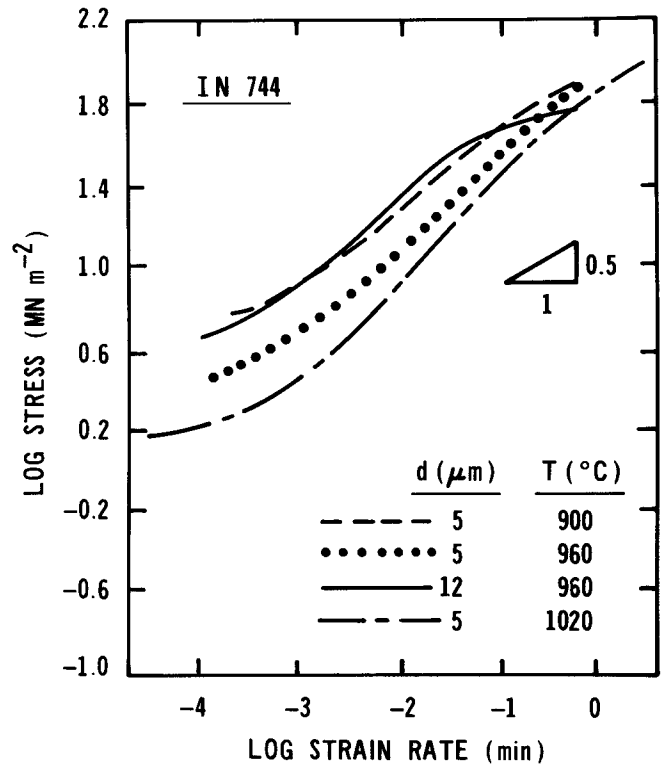


Fig. 3—Double logarithmic plot of stress vs strain rate for IN 744 (after Ref. 56).

Table I. Experimental and Calculated Threshold Stresses for In 744 (56)

Temperature (°K)	Grain Size $\times 10^6$ (m)	$\sigma_0$ Exptl. (MN/m <sup>2</sup> )	$\sigma_0$ Calc <sup>+</sup> (MN/m <sup>2</sup> )	$\Delta\mu$ Calc <sup>++</sup> (MN/m <sup>2</sup> )
1173	5	2.55	0.14	2.87
1233	5	0.98	0.14	1.00
	12	3.14	0.06	3.67
1293	5	0.59	0.14	0.54

<sup>+</sup> $\sigma_0$  calc from Eq. [15]

<sup>++</sup> $\Delta\mu$  calc from Eq. [17]

$G^2/\sigma^2$ ), which is exactly the opposite of what was experimentally observed. Also, according to Eq. [22b],  $\Delta\mu$  will be independent of grain size or will vary inversely with grain size depending upon the flow stress dependence on grain size, *i.e.*,  $\sigma \propto d$  or  $\sigma \propto d^{1/2}$ , respectively. Again, this trend runs counter to the experimental evidence.

The threshold predicted by the Gittus<sup>27</sup> model is independent of grain size and only weakly dependent on temperature through the variation of shear modulus with temperature. The prediction of Eq. [20] is compared with experimental data for IN 744<sup>56</sup> and Pb-Sn eutectic<sup>58</sup> in Table II and values of ledge width,  $L$ , are calculated to fit the experimental data. As can be seen, the calculated ledge widths are too large, of the order of magnitude of the grain size and larger. For the data of Gecklini and Barrett<sup>58</sup> on Pb-Sn, Gittus calculated an  $L$ -value about six times lower ( $L \approx 4 \times 10^{-7}$  m) and concluded that a ledge width to ledge height of about 100 will be required to fit the data. This will result in a ledge height of about  $40 \times 10^{-10}$  m which is several times larger than the boundary width.<sup>59,60</sup> In addition, experimental observations indicate that the height of the boundary ledges of

**Table II. Comparison between Equation [20] and Experimental Results**

Material	Temperature (°K)	Grain Size × 10 <sup>6</sup> (m)	σ <sub>0</sub> Exptl (MN/m <sup>2</sup> )	L <sub>Calc</sub> × 10 <sup>6</sup> (m)
In 744	1173	5	2.55	4.48
	1233	5	0.98	11.00
		12	3.14	3.22
	1293	5	0.59	17.20
Pb-Sn	298	3.6 to 11.7	1.13 <sup>+</sup>	2.26

<sup>+</sup>average value

dislocation character is less than  $59 \times 10^{-10}$  m and, hence, the ratio between the ledge width and ledge height is less than 20. This will lead to typical threshold stresses for most alloys of about  $G/40$  to  $G/140$  which are much too high to be of any relevance to superplasticity.

From the foregoing, it is evident that none of the models for threshold stress proposed in the literature with regard to superplasticity can satisfactorily explain the experimental observations. It is our contention that the effect which is widely interpreted as the operation of a threshold stress can in many instances be due to deformation-enhanced grain growth during superplastic flow.<sup>8,57,61</sup> Concurrent grain growth during deformation will lead to an upswing in the  $\log \sigma - \log \dot{\epsilon}$  curve, especially at low strain rates, as shown convincingly by Rai and Grant<sup>10</sup> and Arieli *et al.*<sup>50</sup> This may lead to apparent impression for the existence of a threshold stress. Figures 4(a) and (b) show the effect of grain size and temperature on the plateau stress at low strain rates for Pb-Sn eutectic.<sup>58</sup> It can be seen from Figures 4(a) and (b) that the plateau (threshold) stress decreases with decreasing grain size and increasing temperature, in agreement with the results of Smith *et al.*<sup>56</sup> for IN 744. There is a tendency for datum points to coalesce into a single line at very low strain rates (lower than those used in that investigation), and this is in agreement with kinetics of concurrent grain growth. The instantaneous grain size,  $d^*$ , during superplastic flow is

\*In the absence of dissociated dislocations the pipe and grain boundary diffusivities are equal.<sup>66</sup>

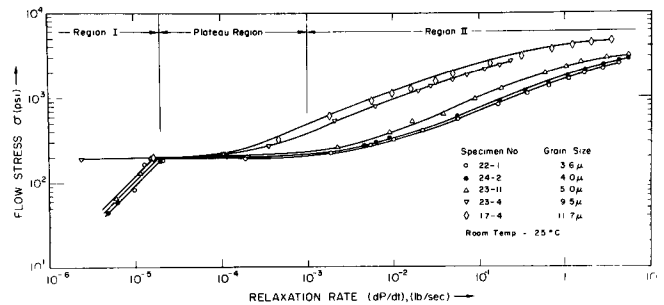
given by<sup>50</sup>

$$d^* = d_0 + \frac{K'}{d^*} (t)^c \exp\left(-\frac{Q_b}{RT}\right) \quad [23]$$

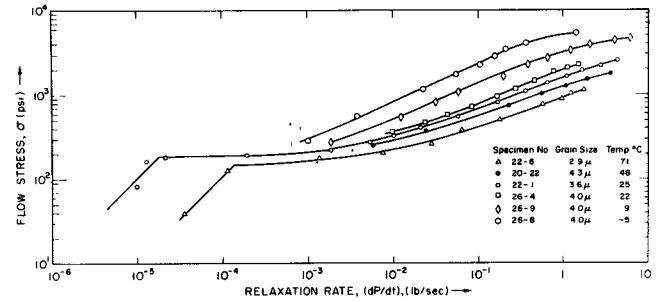
and, hence, the grain growth rate is

$$\frac{\partial (d^*)}{\partial t} = \frac{K' c \exp\left(-\frac{Q_b}{RT}\right)}{(t)^{1-c} (2d^* - d_0)} \quad [24]$$

According to Eq. [24] the smaller grains will grow faster, and the higher the temperature the faster the grain growth rate. Also, at very long testing times the grain growth rate will approach zero, *i.e.*, there will be a limiting grain size, and, hence, the tendency of datum points (Figure 4(b)) to coalesce into a single line at very low strain rates (very long testing times). However, often before the strain rates where a single plateau stress can be observed there is a transition in the deformation mechanism and diffusional creep becomes operative (Figure 4(b)). This behavior strengthens our contention that deformation-enhanced grain growth is responsible for the observed plateau stress region. The



(a)



(b)

Fig. 4—Log  $\sigma$  vs log  $\dot{\sigma}(\alpha\dot{\epsilon})$  for Pb-Sn eutectic at various grain sizes (a) and temperatures (b).

process is shown schematically in Figure 5. The broken lines represent superplastic creep and diffusional creep at two grain sizes  $d_0$  and  $d_1 > d_0$ , respectively. If no grain growth occurs, then the superplastic creep line and diffusional creep ( $d_0$ ) line will describe the deformation behavior over the range of strain rates considered. If, however, the grain growth does occur, then at low strain rates the superplastic creep line will show an upswing and will meet the diffusional creep line at  $d_1$ , which is now the instantaneous grain size due to grain growth. The result is an apparent plateau stress level as depicted in the figure.

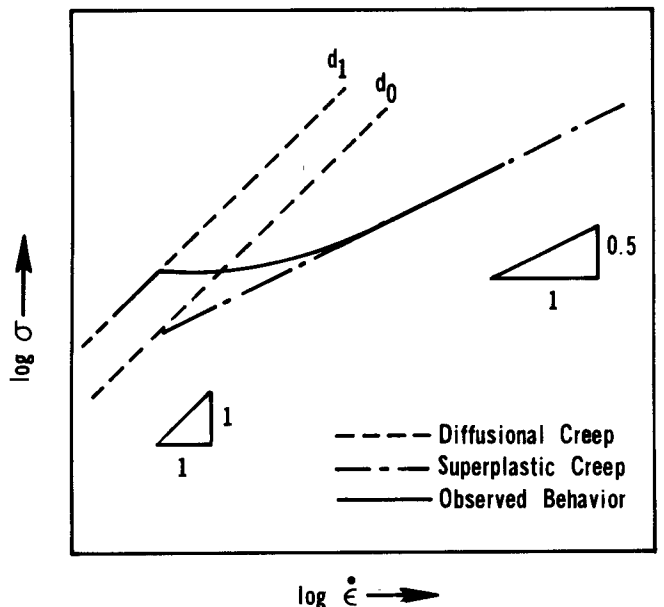


Fig. 5—Schematic representation of the apparent threshold stress due to grain growth.



### (3) Diffusivity

The thermally activated nature of superplastic deformation manifests itself in the temperature dependence of the strain rate. The measured activation energies in Region II of superplasticity generally fall into two categories: activation energies similar to those for grain boundary diffusion<sup>11,14-17,22,48,49,62,63</sup> and those comparable to the energy for lattice diffusion.<sup>9,28,64,65</sup> Two of the models<sup>27,28</sup> were specifically conceived to explain the values of activation energy close to those for lattice diffusion. Hayden *et al*<sup>28</sup> suggested that the rate-controlling diffusion process will change from pipe\* to lattice self-diffusion at a critical temperature at which the two velocities for edge dislocation climb at grain boundaries are equal. However, since the climb process that is envisaged here occurs at a distance of a few angstroms from the grain boundary, it seems more probable<sup>3</sup> that the rate of climb will be controlled by grain boundary diffusion at all temperatures up to the melting point. Gittus<sup>27</sup> proposed that the rate of deformation in superplastic regime is controlled by the interphase diffusivity which takes values closer to those for lattice self-diffusion than those for grain-boundary diffusion. However, in view of the results obtained by Langdon and co-workers<sup>43,44</sup> which show that grain boundaries slide faster than interphase boundaries, the activation energy associated with the faster sliding process, *i.e.*, grain boundary diffusivity, should control the rate of deformation. In the rest of this section we will try to show that in many instances grain-boundary diffusivities of alloys can take on values which are much larger than those for pure base metals, approaching those for lattice self-diffusion in pure metals to which they are usually compared.

(a) *Changes in grain-boundary chemistry.* Figure 6 shows a typical binary phase diagram of two metals A and B. Let's assume that we investigate an AB alloy having the nominal composition  $x_B$  pct of B and  $(100 - x)$  pct of A. The activation energy for deformation is determined by measuring the strain rate under constant applied stress at temperatures  $T_1, T_2, T_3$ , and  $T_4$  ( $T_4 > T_3 > T_2 > T_1$ ). A plot of  $\ln(\dot{\epsilon} G^{n-1} T)$  vs  $1/T$  will yield the activation energy for energy, from the slope of the plot, *i.e.*,

$$Q = R \frac{\partial \ln(\dot{\epsilon} G^{n-1} T)}{\partial (1/T)} \Big|_{\sigma, \text{ structure, chemistry}} \quad [25]$$

where  $R$  = gas constant.

However, inspection of phase diagram in Figure 6 indicates that the chemistry of both  $\alpha$  and  $\beta$ -phases changes with variations in temperature. At  $T_1, T_2, T_3$ , and  $T_4$  the content of A in  $\beta$ -phase is  $a_1, a_2, a_3$ , and  $a_4$  ( $a_4 > a_3 > a_2 > a_1$ ), respectively, while the content of B in  $\alpha$ -phase is  $b_1, b_2, b_3$ , and  $b_4$  ( $b_1 > b_2 > b_3 > b_4$ ), respectively. Such variations in the solute content<sup>60</sup> might affect either the pre-exponential factor ( $D_0$ ) or the activation energy ( $Q$ ) or both. Tables III and IV list the measured activation energy and the preexponential factor of grain boundary diffusion of Zn in Sn and Sn in Zn<sup>67</sup>, and Figures 7 and 8 show the observed activation energy and the calculated diffusivities as a function of Zn-content, respectively. The calculated diffusivities for three temperatures are summarized in Table V. It is evident from Figures 7 and 8 and Tables III through V that

**Table III. Grain Boundary Diffusion of Zn in Sn-Zn Alloys**

Zn (At. Pct)	$D_0 (\text{M}^2/\text{s}) \times 10^4$	$Q$ (kJ/mol)
8.6	16.2	54.0
18.1	0.8	47.3
38.4	8.0	58.0
86.0	5.5	62.8
100.0	0.11	54.4

**Table IV. Grain Boundary Diffusion of Sn in Sn-Zn Alloys**

Zn (At. Pct)	$D_0 (\text{M}^2/\text{s}) \times 10^4$	$Q$ (kJ/mol)
0.0	0.064	40.0
0.9	0.48	48.1
8.6	0.12	46.9
18.1	0.036	43.9
24.3	0.19	49.8
38.4	0.19	51.5
68.5	5.0	62.8
86.0	10.4	66.1

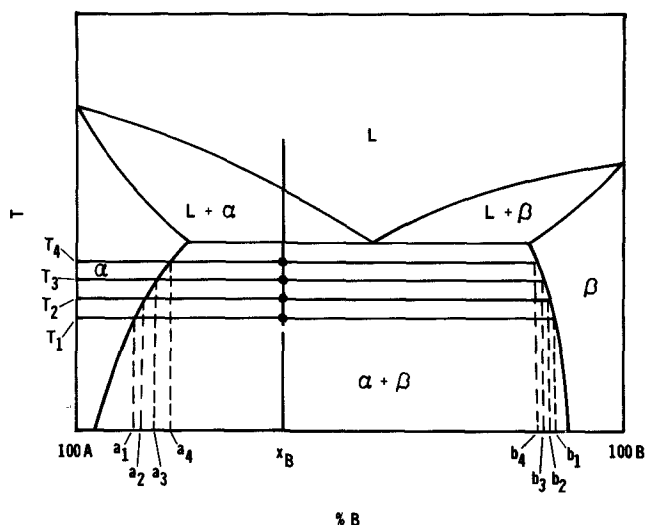


Fig. 6—Typical binary phase diagram.

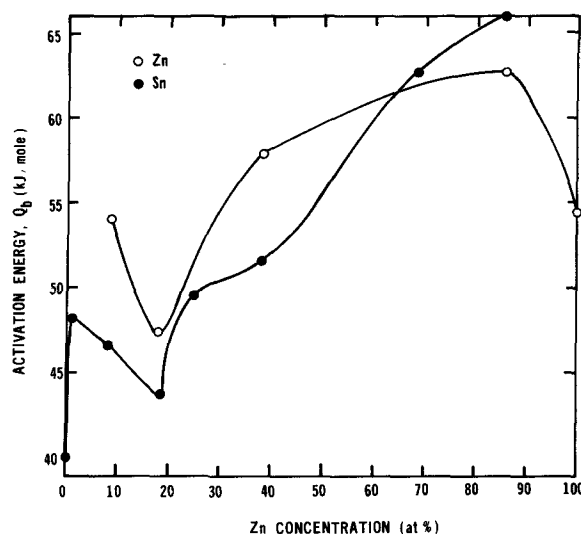


Fig. 7—Activation energy vs Zn concentration.

Table V. Grain Boundary Diffusivities of Zn in Sn and Sn in Zn

Zn (At. Pct)	$D_b\text{Zn} \text{ (m}^2\text{/s)}$			$D_b\text{Sn} \text{ (m}^2\text{/s)}$		
	300 K	375 K	450 K	300 K	375 K	450 K
0				$7.83 \times 10^{-13}$	$1.89 \times 10^{-11}$	$1.58 \times 10^{-10}$
0.9				$2.28 \times 10^{-13}$	$1.05 \times 10^{-11}$	$1.35 \times 10^{-10}$
8.6	$7.45 \times 10^{-13}$	$5.49 \times 10^{-11}$	$9.65 \times 10^{-10}$	$9.38 \times 10^{-14}$	$3.92 \times 10^{-12}$	$4.73 \times 10^{-11}$
18.1	$5.3 \times 10^{-13}$	$2.29 \times 10^{-11}$	$2.82 \times 10^{-10}$	$9.04 \times 10^{-14}$	$2.99 \times 10^{-12}$	$3.09 \times 10^{-11}$
24.3				$4.63 \times 10^{-14}$	$2.44 \times 10^{-12}$	$3.44 \times 10^{-11}$
38.4	$7.55 \times 10^{-14}$	$7.64 \times 10^{-12}$	$1.66 \times 10^{-10}$	$2.38 \times 10^{-14}$	$1.43 \times 10^{-12}$	$2.20 \times 10^{-11}$
68.5				$6.94 \times 10^{-15}$	$1.03 \times 10^{-12}$	$2.89 \times 10^{-11}$
86.0	$7.64 \times 10^{-15}$	$1.13 \times 10^{-12}$	$3.18 \times 10^{-11}$	$3.81 \times 10^{-15}$	$7.38 \times 10^{-13}$	$2.47 \times 10^{-11}$
100.0	$4.28 \times 10^{-15}$	$3.26 \times 10^{-13}$	$5.86 \times 10^{-12}$			

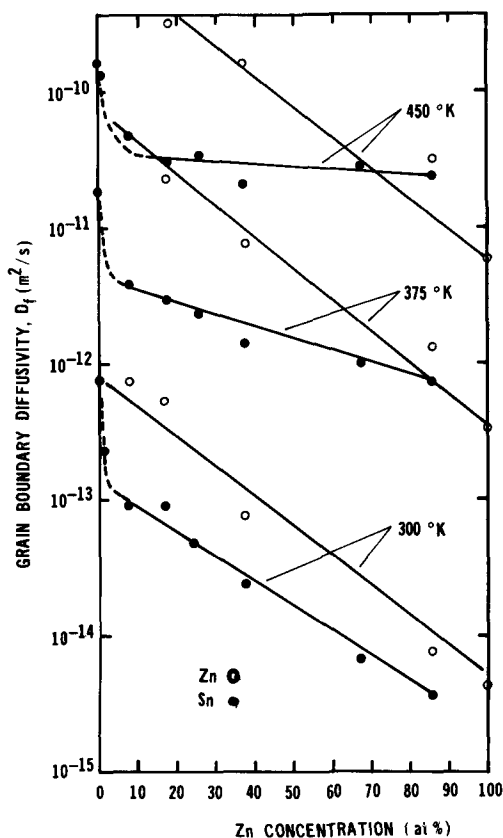


Fig. 8—Diffusivity vs Zn concentration.

although the diffusivities decrease with increasing Zn content in the alloy, large variations in the measured activation energies can be observed. For example, the activation energy for grain boundary diffusion of Sn in Zn at 18.1 at. pct Zn is 0.66 of that at 86 at. pct Zn, which in turn is close to that for grain boundary self-diffusion in pure Zn parallel

to the c-axis, *i.e.*,  $Q = 79.5 \text{ kJ/mol}$ .<sup>68</sup> In addition, the grain-boundary diffusivity might be either enhanced or reduced by the presence of impurity solute-atoms in the grain-boundaries.<sup>60</sup> For example, Juve-Duc *et al*<sup>69</sup> have shown that reducing the impurity level in an austenitic steel (18 pct Cr and 10 pct Ni) from 560 ppm to 5 ppm will have little effect on the activation energy for lattice self-diffusion but will dramatically increase the activation energy for grain-boundary self-diffusion (Table VI). These authors explain their results by eventual variations of both grain-boundary chemistry and grain-boundary structure with changes in temperature. This corresponds with an explanation put forward by Rosenberg<sup>70</sup> for the solute effect based on the interaction between solute atoms and the grain-boundary defects. At a given grain-boundary structure, solute-atoms<sup>73</sup> might affect the grain boundary diffusivity either by changing the atomic jump frequencies along the grain-boundary or by influencing the exchange of atoms between the grain-boundary and the lattice.

(b) *Changes in grain-boundary structure and grain-boundary precipitation.* Grain-boundaries in metallic materials invariably contain intrinsic grain-boundary dislocations (IGBD) which are part of the boundary geometry and topographical defects such as steps, ledges, discontinuities, and so forth, which are formed during processing.<sup>71</sup> In addition, during plastic deformation lattice dislocations “run-in” the boundary, dissociate, and form extrinsic grain-boundary dislocations (EGBD). The EGBD’s in the boundary will interact with the IGBD’s and the topographical defects, creating localized high strain energy regions which are preferential sites for nucleation and growth of grain-boundary precipitates.<sup>71</sup> The effect which such boundary precipitate might have on the grain-boundary diffusion was shown in the work of Delannay, Huntz, and Lacombe.<sup>72</sup> Investigating an 80 pct Ni-20 pct Cr alloy in the temperature range between 1123 K and 1473 K (850 °C and 1200 °C), they observed at temperatures above ~1323 K

Table VI. The Effect of Impurity Solute-Atom Content on the Activation Energy for Self-Diffusion (after Ref. 69)

	18-10 Austenitic Steel 5 ppm Impurities	18-10 Austenitic Steel 560 ppm Impurities	$\gamma$ -Iron 99.99 Pct
Activation energy for lattice self-diffusion, $Q$ [kJ/mol]	280	213	255
Preexponential factor for lattice self-diffusion, $D_0$ [m <sup>2</sup> /s]	$4.4 \times 10^{-5}$	$1.6 \times 10^{-7}$	$4 \times 10^{-6}$
Activation energy for grain-boundary self-diffusion, $Q_b$ [kJ/mol]	193	75	155
Factor $P_f$ for grain boundary self-diffusion [m <sup>3</sup> /s]*	$3.6 \times 10^{-14}$	$8.3 \times 10^{-18}$	$3.8 \times 10^{-14}$

\* $P_f = D_b \delta \alpha$ , where  $\delta$  = grain-boundary width and  $\alpha$  = segregation coefficient for solvent.

(1050 °C) preferential precipitation of Cr<sub>23</sub>C<sub>6</sub> carbide at grain-boundaries. Associated with the carbide precipitation at grain-boundaries was a dramatic change in the value of the activation energy for grain-boundary diffusion, while the activation energy for lattice-diffusion remained unchanged. Their results for <sup>51</sup>Cr diffusion are summarized in Table VII.

(c) *Correlation*. If the dependence of steady-state strain rate during superplastic flow on stress, temperature, and grain size is expressed as

$$\frac{\dot{\epsilon} k T}{D_0 G b} \exp\left(\frac{Q}{RT}\right) = A \left(\frac{b}{d}\right)^p \left(\frac{\sigma}{G}\right)^n \quad [26]$$

then by applying logarithms on both sides of Eq. [26] we obtain

$$\ln\left(\frac{\dot{\epsilon} d^p k T}{A D_0 G b^{p+1}}\right) + \frac{Q}{RT} = n \ln\left(\frac{\sigma}{G}\right) \quad [27]$$

Eq. [27] indicates that if *n* and *p* are constants and take the same values for all superplastic materials, then a plot of  $\ln(\sigma/G)$  vs  $Q/RT$  at  $\dot{\epsilon} d^p = \text{constant}$  will yield a straight line. Such a plot for several superplastic alloys is shown in Figure 9 for  $\dot{\epsilon} d^2 = 2.9 \times 10^{-11} \text{ cm}^2$  per second. The data fall onto two almost parallel lines and segregates according to the diffusivity, *e.g.*, either lattice or grain-boundary. The major difference between the two groups is the value taken by the intercept which, according to Eq. [27], is given by

$$\text{Intercept} = 2.3 \log\left(\frac{\dot{\epsilon} d^2 k T}{A D_0 G b^3}\right) \quad [28]$$

For the superplastic alloys used in Figure 9,  $kT/Gb^3$  changes very little and, therefore, the difference in the intercept value is due to the values taken by *A* and *D*<sub>0</sub>. The pre-exponential factor *D*<sub>0</sub> has been shown in this section to be sensitive to grain-boundary chemistry and structure and, as will be shown in the next section, the parameter *A* is dependent on the same factors. Hence, we might infer that due to changes in grain-boundary chemistry and/or structure, the deformation of several superplastic materials is controlled by grain boundary diffusivities having values that are numerically close to that for lattice self-diffusion for those pure metals which constitute the major alloying element for such materials. This suggestion is admittedly debatable at present. More precise values of grain boundary diffusivity at specific alloy compositions are required before a definite conclusion can be drawn.

#### (4) Summary

(a) It is shown that it is not necessary to model the stress/strain rate behavior in such a way as to explain the variation of the strain rate sensitivity coefficient with strain

**Table VII. <sup>51</sup>Cr Diffusivity in an 80 Pct Ni-20 Pct Cr Alloy (after Ref. 72)**

	Temperature, <i>T</i> (K)	
	<i>T</i> < 1323 K	<i>T</i> > 1323 K
<i>Q</i> <sub>i</sub> [kJ/mol]	264	264
<i>D</i> <sub>0i</sub> [m <sup>2</sup> /s]	2.2 × 10 <sup>-3</sup>	2.2 × 10 <sup>-3</sup>
<i>Q</i> <sub>b</sub> [kJ/mol]	251	151
<i>D</i> <sub>0b</sub> [m <sup>2</sup> /s]	—	1.3 × 10 <sup>-13</sup>

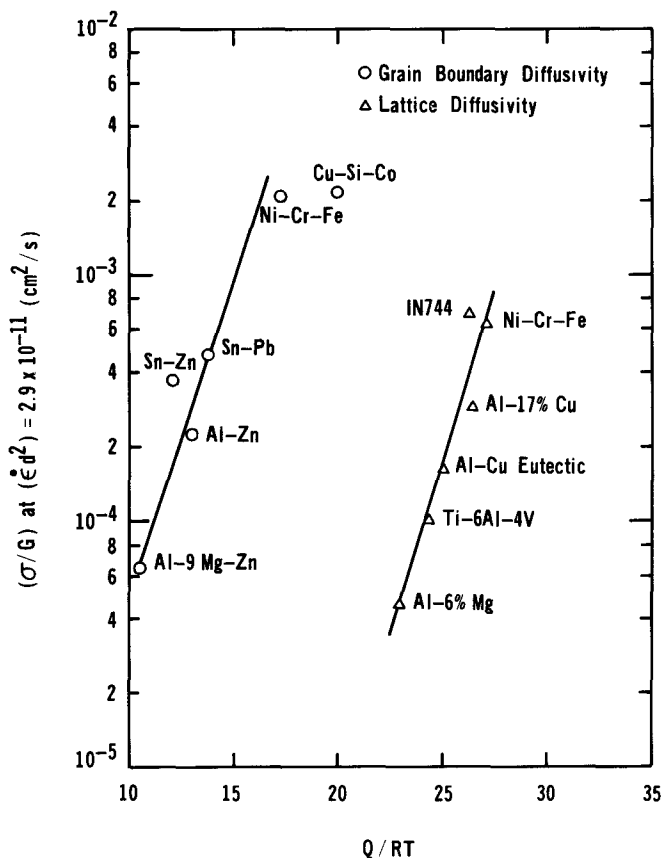


Fig. 9—Normalized plot of  $(\sigma/G)$  vs  $Q/RT$ .

rate. The *m*-values determined from strain rate change experiments which show such dependence are related to the mechanics of the plastic flow but not to the micromechanism of the plastic flow.

(b) None of the proposed models for threshold stress mechanisms can explain the experimental data. It is suggested that in many instances concurrent grain growth during deformation can rise to an apparent threshold stress.

(c) The identification of the rate-controlling diffusion process during superplastic flow is extremely difficult due to both the complexity of the grain-boundary diffusion processes and the scarcity of data regarding the grain-boundary diffusion in alloys. The values of activation energy for grain-boundary diffusion in alloys are, in many cases, numerically close to those for lattice diffusion for pure base metals. More careful investigations are needed in order to establish if some of the reported and comparatively higher activation energy values for superplasticity truly correspond to that for lattice diffusion.

#### C. Additional Considerations

##### (1) Dislocation Pile-ups at and in the Grain-Boundaries

Spingarn and Nix<sup>29</sup> were the first to suggest that in the models for superplasticity at high temperatures, the grain-boundaries are unable to sustain the stress concentrations resulting from dislocation pile-ups.

Gifkins<sup>25</sup> calculated that the stress at the head of the dislocation pile-up,  $\sigma_p$ , is given by

$$\sigma_p = \frac{\sigma^2 d}{G b} \quad [29]$$

This stress cannot exceed the stress,  $\sigma_f$ , for each crack formation, *e.g.*,<sup>74</sup>

$$\sigma_f = \left[ \frac{96 G \gamma}{\pi d (1-\nu)} \right]^{1/2} \quad [30]$$

Equating Eqs. [29] and [30] the critical applied stress,  $\sigma_{cr}$  (*i.e.*, the applied stress which cannot be exceeded without crack formation) is given by

$$\sigma_{cr} = \left[ \frac{96 G^3 b^2 \gamma}{d^3 \pi (1-\nu)} \right]^{1/4} \quad [31]$$

Eq. [31] was used to calculate  $\sigma_{cr}$  for several superplastic alloys which Gifkins compared with the prediction from his model.<sup>25</sup> The results are listed in Table VIII together with the approximate minimum value of stress where Region II is still observed,  $\sigma_{II \text{ min}}$ . Similar calculations performed for dislocation pile-ups inside the grains<sup>22,23</sup> revealed that for a typical superplastic material the number of dislocations in a pile-up which a grain-boundary can sustain is between three and eight. Hence, it seems very likely that in the context of accommodation process involving dislocation motion, it is the climb of individual dislocations<sup>28,29,30</sup> that will control the rate of deformation and not climb from piled-up dislocation arrays.

## (2) Grain-Boundary Structure

In the course of this paper we have seen that grain-boundary structure and grain-boundary processes dependent

Table VIII.  $\sigma_{cr}$ -Values

Alloy	Ref.	$\sigma_{cr}$ (MPa)	$\sigma_{II \text{ min}}$ (MPa)
Sn-Pb eutectic	75	4.48	≈ 10
Zn-22 pct Al	49	41.30	≈ 80
Zn-0.2 pct Al	76	52.70	≈ 110
Pb-2.5 pct Tl	25	3.39	≈ 3
Cu-2.8 pct Al-1.8 pct Si-0.43 pct Co	40	58.58	≈ 50

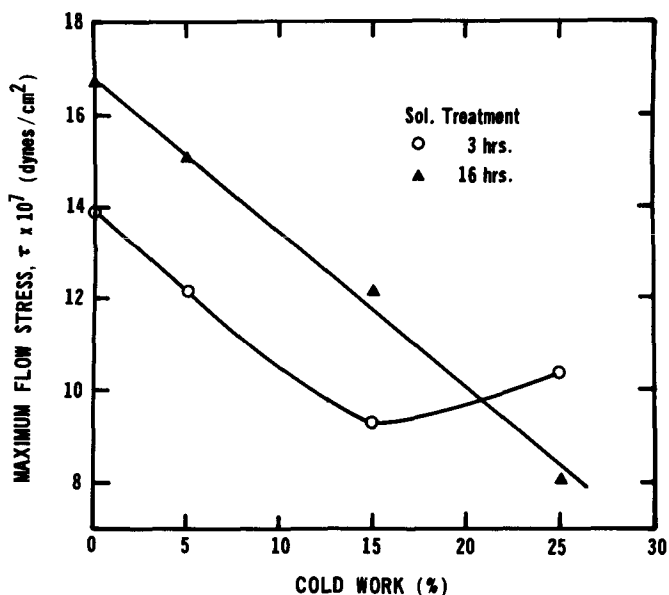


Fig. 10—The effect of prior cold work and thermal treatments on the flow stress of Zn-22 pct Al eutectoid.

on its structure such as grain-boundary precipitation will have a major influence on diffusivity, on the magnitude and nature of the threshold stress for deformation, and undoubtedly on grain-boundary sliding and migration.<sup>60,71,77,78</sup> Therefore, it is important to consider changes in the grain boundary structure which might affect the superplastic behavior of metals and alloys. For example, large variations in the flow shear stress,  $\tau$ , with both the amount of cold work and the time at the solution treatment temperature were observed for a Zn-22 pct Al alloy with a grain size of  $1.7 \times 10^{-4}$  cm and tested at 503 K and  $\dot{\gamma} = 1.88 \times 10^{-2} \text{ s}^{-1}$  (Figure 10). Venkatesh and Murr<sup>79</sup> measured the ledge density in the grain-boundaries of a 99.9999 pct Al as a function of thermomechanical treatments (Table IX). They observed that the larger the number of lattice dislocations which intersect with the grain-boundaries, the more apparent will be the ledge structure in the grain-boundary as seen under the TEM. Furthermore, the larger the number of lattice dislocations generated by a particular thermomechanical treatment, the larger the ledge density (Table IX). Similar observations were made by Tangri and Malis<sup>81</sup> for pure nickel.

Studies of grain-boundary ledges<sup>80</sup> show that the ledge density is sensitive to the boundary misorientation. Various thermomechanical treatments will result in different distributions of the boundary misorientation.<sup>80</sup> Tangri and Malis<sup>81</sup> report that for pure nickel the grain-boundary defect density decreases as the grain size decreases. Recently, Varin and Tangri<sup>82</sup> studied the effect of grain growth during annealing experiments in a high purity (0.01 wt pct C) austenitic stainless steel on the spreading temperature,  $T_d$ , of extrinsic grain-boundary dislocations (*i.e.*, “run-in” lattice dislocations). They found that during grain growth the average spreading temperature was 83 K higher than the average spreading temperature for fully recrystallized specimens. Since the low carbon content in their alloy makes the variations in carbon concentration at grain-boundaries (after grain growth and recrystallization treatments, respectively) very unlikely, they conclude that a marked difference in the grain-boundary structure following grain growth is responsible for the observed differences.

We can try to correlate some of the above results with observations of superplastic behavior of metals and alloys. Grivas<sup>83</sup> investigated the effect of thermomechanical treatments on the value of the substructure related parameter (A) in the constitutive equation for superplastic flow of a Sn-Pb

Table IX. Effect of Thermomechanical Treatments (Pure Aluminum, after Ref. 79)

Thermomechanical Treatment	Ledge Density Number Micron
1. Annealing	
slow cooling	0.1
fast cooling	0.2
very fast cooling	0.6
2. Cold-Rolling	
6 pct	0.1
18 pct	0.3
50 pct	0.5
3. Creep	
$\sigma = 3$ MPa	0.2
$\sigma = 6$ MPa	0.5
$\sigma = 12$ MPa	4.0

eutectic alloy. He found that for specimens prepared from the same ingot but receiving different mechanical treatments, the  $A$ -value increased with an increase in the amount of plastic reduction at room temperature (Table X). The results shown in Table X exhibit the same trend as the ledge density values following cold-rolling (Table IX).

Only one model<sup>30</sup> attempts to incorporate features pertinent to the grain-boundary structure or the substructure in general. A relation between the sliding unit,  $h$ , in Eq. [13] and grain-boundary ledge density can be seen as follows. Extrinsic grain-boundary dislocations can move in the boundary, giving rise to grain-boundary sliding.<sup>84</sup> The unit of sliding will then be equal to the average interdistance between the adjacent ledges in the boundary. An increase in the ledge density will decrease  $h$  and will increase  $A$  (Eq. [13]). Support for the view that  $A$ -values are mainly related to the grain-boundary structure is obtained from work in progress in our laboratory<sup>85</sup> which strongly indicates that cold-working a Ti-6Al-4V alloy for various amounts prior to grain growth anneal will result in increases in  $A$ -value in Region II but will leave  $A$ -values in Region III (which are controlled by grain interior structure) essentially unchanged. Such variation of the value of the parameter  $A$

**Table X. The Effect of Mechanical Working on A-Values for Sn-Pb Eutectic Alloy (after Ref. 83)**

Initial Diameter $\times 10^2$ (m)	Final Diameter $\times 10^2$ (m)	Reduction (Pct)	A-Value
5.08	2.22	80 pct	2000
3.81	2.22	66 pct	800
2.54	2.22	24 pct	100

depending on prior thermomechanical history has important implication on the transition from the superplastic mechanism to the appropriate rate controlling mechanism in Region I. Thus, nominal similarity in the chemical composition and grain size are often not adequate to characterize a superplastic material completely. At the same temperature and strain rate, the resultant flow stress in Region I may still differ between two groups of researchers<sup>16,61,63,83</sup> because of possible differences in the parameter  $A$ , which incorporates some of the details of inherited grain boundary substructure and its chemistry. As explained earlier, possibility of grain growth in low strain rate Region I adds further to this discrepancy.

Finally, the fact that the grain-boundary defect density increases as the grain size increases,<sup>81</sup> as well as the fact that the grain-boundary structure seems to change markedly during grain growth treatments,<sup>82</sup> might be the reason for the experimentally observed strong grain size dependence of the strain rate within superplastic regime.

### (3) Summary

(a) Grain-boundaries cannot support the stress concentrations resulting from the dislocation pile-ups in the boundary under the applied flow stresses usually encountered in superplastic region.

(b) During GBS, the accommodation process due to dislocation motion is very likely associated with motion of individual dislocations and not with dislocations from piled-up arrays.

(c) The grain-boundary structure is very sensitive to thermomechanical treatments and, in turn, the superplastic behavior seems to be related to the grain-boundary structure.

**Table XI. Summary of the Comparison of Various Models for the Rate-Controlling Deformation Mechanisms with Experiment Theoretically Predicted**

	Experimentally Required	Ashby- Verall <sup>21</sup>	Ball-Hutch- inson <sup>22</sup> + Mukherjee <sup>23</sup>	Mukherjee <sup>24</sup>	Gifkins <sup>25,26</sup>	Gittus <sup>27</sup>	Hayden <i>et al</i> <sup>28</sup>	Spingarn- Nix <sup>29</sup>	Arieli- Mukherjee <sup>30</sup>
<b>1. Microstructural</b>									
a. Grain-boundary sliding	Yes	Yes	Yes	Yes	Yes	Yes	Yes	Yes	Yes
b. Grain-boundary migration	Yes	*	*	*	*	*	*	*	Yes
c. Equiaxed grain shape	Yes	Yes	Yes	Yes	Yes	Yes	Yes	Yes	Yes
d. Grain rotation	Yes	Yes	*	Yes	Yes	*	*	*	Yes
e. 3-D grain rearrangement	Yes	*	*	*	Yes	*	*	*	Yes
f. Dislocation activity	Yes	*	Yes	Yes	*	*	Yes	Yes	Yes
g. Dislocation pile-ups	No	No	Yes	Yes	Yes	Yes	No	No	No
i. Grain-boundary structure related details	Yes	No	No	No	No	No	No	No	Yes
<b>2. Phenomenological</b>									
a. $m = f(\dot{\epsilon})$	No	Yes	No	No	No	Yes	No	Yes	No
b. Grain-boundary diffusion	Yes	Yes	Yes	Yes	Yes	No	Yes	Yes	Yes
c. Lattice self-diffusion	No	Yes	No	No	No	Yes <sup>+</sup>	Yes	No	No
d. Threshold stress	No	Yes	No	No	No	Yes	No	No	No

\*Not predicted in the original paper but can be accounted for through grain-boundary sliding (see text – Section IV-A for discussion).

<sup>+</sup>Interphase diffusion

## V. FINAL SUMMARY AND CONCLUSIONS

1. The basic prerequisites for the manifestation of micro-grain superplasticity are now well understood: a fine, equiaxed and fairly stable grain structure, a temperature equal to or higher than half the melting point in absolute degrees, and a value of the strain rate sensitivity parameter approximately equal to 0.5.
2. The dominant microscopic process in superplasticity is grain boundary sliding (GBS). When a superplastic specimen plastically deforms under stress, the specimen changes shape. The shape change is brought about by GBS and grain rotation. The specific micromechanism that accommodates the stresses generated at triple points due to GBS is the rate-controlling step.
3. The superplastic model for GBS with diffusional accommodation (Ashby-Verall) has attractive features and explains topological features well. However, some of the mechanical predictions of the model, *e.g.*, a gradual transition of the stress dependence of the strain rate, the magnitude, the temperature and grain size dependence of the threshold stress, the variation in the grain size dependence of the strain rate, and a variable value of the activation energy for the superplastic deformation often are not in agreement with experimental results. However, this model was the first to open the way for more realistic consideration of the process of grain rearrangement that typify superplastic deformation.

Models that describe accommodation process involving dislocation pile-ups within the grains can describe the stress and grain size dependence of strain rate in superplasticity reasonably well. However, it is extremely unlikely that grain boundaries can support the stress concentrations resulting from such pile-ups under the stresses and temperatures usually encountered in superplasticity. The models that invoke accommodation due to dislocation pile-ups at grain or interphase boundaries fare somewhat better. The most noteworthy ones are due to Gifkins<sup>25,26</sup> and Gittus.<sup>27</sup> The latter model specifically considers two-phase material, and the activation energy for superplasticity is that for interphase diffusion.

Among models for accommodation of GBS due to motion of individual dislocations, that due to Hayden *et al.*<sup>28</sup> predicts a transition in activation energy from pipe to lattice diffusion as a function of temperature, which is contrary to experimental observations. The model by Spingarn and Nix<sup>29</sup> depicts superplasticity as a transition region with variable values for stress and grain size dependence of the strain rate. The activation energy given is that for grain boundary diffusion. As presently formulated, this model does not take into account the important topological features in superplasticity, *i.e.*, neighbor-switching events or equiaxed grain shape after extensive strain, and so forth. A more recent model by Arieli and Mukherjee<sup>30</sup> considers individual lattice dislocations in a narrow region near the interfaces that climb directly into or along the interfaces. The model takes into consideration the grain boundary structure and suggests that the substructure related parameter in the equation for superplastic strain rate will vary both with interface structure and the structure in the narrow zone near the interface. It

also incorporates the effect of grain boundary migration on the strain rate. Although some of these substructural parameters in this model need further experimental confirmation, the basic predictions of the model are in accord with experimental observations.

4. The major microstructural characteristics in superplasticity are: extensive grain boundary sliding and migration that vary with type of interface, grain rotation and three-dimensional grain rearrangement, maintenance of essentially equiaxed shape even after considerable plastic deformation, significant strain-induced concurrent grain growth in many systems, and substantial dislocation activity, the extent of which can vary from grain to grain. Not all of the models for superplasticity explicitly account for these microstructural observations. However, the assumption that grain boundary sliding is the dominant deformation mechanism in two-phase materials in superplasticity leads to the implicit inclusion of some of these microstructural characteristics in the models.
5. It is suggested that, for the identification of specific micromechanisms for deformation, the strain rate sensitivity parameter,  $m$ , should be determined from log stress vs log strain rate plot. The  $m$ -values determined from cross-head velocity change type of experiments are more closely related to the mechanics of plastic flow and resistance to necking aspects.
6. None of the proposed models for threshold stress can explain the experimental data well. An alternate suggestion in the literature, *e.g.*, in many instances concurrent grain growth during superplastic deformation can also give rise to an apparent threshold stress, has not been emphasized enough.
7. The scarcity of data on the activation energy of grain boundary diffusion in alloys makes the process of identification of the rate-controlling diffusional process in superplasticity rather difficult. Most of the experimental data suggests that the activation energy in superplasticity is equal to that for grain boundary diffusion. However, often very small changes in impurity or solute atoms can make vast changes in the actual value for grain boundary diffusivity. More careful investigations are needed in order to establish if some of the reported and comparatively higher activation energy values for superplasticity indeed correspond to that for lattice diffusion.
8. The prior thermal and mechanical history of the specimens can produce very large differences in the mechanical results in superplasticity. Such large differences, in spite of nominal similarity in chemical composition and grain size, is very likely due to alteration in the significant details of grain boundary substructure (and possibly its chemistry) during the prior processing history. This aspect needs to be investigated in more detail in future experimental investigations.

## LIST OF SYMBOLS

$a$	constant in grain growth equation
$A$	substructure related parameter in the constitutive equation for high-temperature deformation

## REFERENCES

$b$	Burgers vector
$c$	time exponent in the equation for the grain growth kinetics
$d, d_0, d^*$	grain size, initial grain size, and instantaneous grain size, respectively
$D_0, D_{0b}, D_{0l}, D_{0p}$	preexponential factor, preexponential factor for grain-boundary diffusion, preexponential factor for lattice diffusion, preexponential factor for pipe diffusion, respectively
$D, D_b, D_l, D_p, D_{IPB}$	diffusivity, grain-boundary diffusivity, lattice self-diffusivity, pipe diffusivity, and interphase-boundary diffusivity, respectively
$\delta$	grain boundary width
$E$	line energy per unit length
$\varepsilon$	true tensile strain
$\dot{\varepsilon}$	true tensile strain rate
$G$	shear modulus
$\Gamma$	grain-boundary free energy per unit area
$\dot{\gamma}$	true shear strain rate
$h$	parameter related to the sliding unit distance
$k$	Boltzmann's constant
$K$	empirical parameter, $f(d, m, T, \text{structure, material})$ , in semi-empirical equation $\sigma = K \dot{\varepsilon}$
$K'$	empirical parameter, $f(d, T, \text{structure, material})$ , in semi-empirical equation $\sigma = K' \dot{\varepsilon}^m$
$L$	
$m$	strain rate sensitivity coefficient, $= 1/n$
$M$	grain-boundary mobility
$\Delta\mu$	interface potential
$n$	stress sensitivity coefficient, $= 1/m$
$\omega$	proportionality factor related to the average radius of curvature of curved dislocations
$\Omega$	atomic volume
$p$	grain size dependence of strain rate coefficient
$T, T_M, T_C$	absolute temperature, absolute melting temperature, and absolute critical temperature, respectively
$\sigma, \sigma_0, \sigma_p, \sigma_f, \sigma_{cr}$	true tensile stress, threshold tensile stress, tensile stress at the head of a dislocation pile-up, fracture stress, and critical stress, respectively
$\tau$	true shear stress
$t$	time
$Z$	cut-off distance
$Q, Q_b, Q_l, Q_p$	activation energy, activation energy for grain-boundary diffusion, activation energy for lattice diffusion, and activation energy for pipe diffusion, respectively
$\theta$	grain-boundary misorientation

## ACKNOWLEDGMENTS

This research is supported by a grant no. DE AT03-79ER 10508 of the Division of Materials Sciences, Office of the Basic Energy Sciences, Department of Energy.

1. R. H. Johnson: *Metall. Rev.*, 1970, vol. 15, p. 115.
2. G. J. Davies, J. W. Edington, C. P. Cutler, and K. A. Padmanabham: *J. Mat. Sci.*, 1970, vol. 5, p. 1091.
3. J. W. Edington, K. N. Melton, and C. P. Cutler: *Prog. Materials Science*, 1976, vol. 21, p. 61.
4. T. H. Alden: in "Treatise on Materials Science and Technology," R. J. Arsenault, ed., Academic Press, New York, NY, 1975, vol. 6, p. 226.
5. A. K. Mukherjee: *Ann. Rev. Mater. Sci.*, 1979, vol. 9, p. 191.
6. D. M. R. Taplin, G. L. Dunlop, and T. G. Langdon: *ibid.*, p. 151.
7. A. Arieli and A. K. Mukherjee: Proceedings of the Conference on "Micromechanisms for Plasticity and Fracture in Engineering Solids," Oxford, England, 1980, to be published by Pergamon Press.
8. A. Arieli and A. K. Mukherjee: *Mater. Sci. and Engr.*, 1980, vol. 45, p. 61.
9. H. W. Hayden, R. C. Gibson, H. F. Merrick, and J. H. Brophy: *Trans. ASM*, 1967, vol. 60, p. 3.
10. G. Rai and N. J. Grant: *Metall. Trans. A*, 1975, vol. 6A, p. 385.
11. S. T. Lam, A. Arieli, and A. K. Mukherjee: *Mater. Sci. Eng.*, 1979, vol. 40, p. 73.
12. A. Arieli and A. Rosen: *Metall. Trans. A*, 1977, vol. 8A, p. 1591.
13. H. W. Hayden and J. H. Brophy: *Trans. ASM*, 1968, vol. 61, p. 542.
14. M. L. Vaidya, K. L. Murty, and J. E. Dorn: *Acta Metall.*, 1973, vol. 21, p. 1615.
15. S. C. Misro and A. K. Mukherjee: in "Rate Processes in Plastic Deformation," J. C. M. Li and A. K. Mukherjee, eds., ASM, Metals Park, OH, 1975, p. 434.
16. A. Arieli, A. K. S. Yu, and A. K. Mukherjee: *Metall. Trans. A*, 1980, vol. 11A, p. 181.
17. A. Arieli and A. K. Mukherjee: *Acta Metall.*, 1980, vol. 10, p. 1571.
18. J. E. Bird, A. K. Mukherjee, and J. E. Dorn: in "Quantitative Relation Between Properties and Microstructure," D. G. Brandon and A. Rosen, eds., Israel Universities Press, Jerusalem, 1969, p. 255.
19. W. Beere: *J. Mater. Sci.*, 1977, vol. 12, p. 2093.
20. M. F. Ashby: *Surface Sci.*, 1972, vol. 31, p. 498.
21. M. F. Ashby and R. A. Verall: *Acta Metall.*, 1973, vol. 21, p. 149.
22. A. Ball and M. M. Hutchinson: *Met. Sci. J.*, 1969, vol. 3, p. 1.
23. A. K. Mukherjee: *Mater. Sci. Eng.*, 1971, vol. 8, p. 83.
24. A. K. Mukherjee: in "Grain Boundaries in Engineering Materials," J. L. Walter *et al.*, eds., Claitor Publishing, Baton Rouge, LA, 1975, p. 93.
25. R. C. Gifkins: *Metall. Trans. A*, 1976, vol. 7A, p. 1225.
26. R. C. Gifkins: *J. Mater. Sci.*, 1978, vol. 13, p. 1926.
27. J. H. Gittus: *Trans. ASME, J. Eng. Mater. Technol.*, 1977, vol. 99, p. 244.
28. H. W. Hayden, S. Floreen, and P. D. Goodell: *Metall. Trans.*, 1972, vol. 3, p. 833.
29. J. R. Spingarn and W. D. Nix: *Acta Metall.*, 1979, vol. 27, p. 171.
30. A. Arieli and A. K. Mukherjee: *Mater. Sci. Eng.*, 1980, vol. 45, p. 61.
31. J. Weertman: *Trans. ASM*, 1968, vol. 61, p. 681.
32. A. K. Mukherjee, J. E. Bird, and J. E. Dorn: *Trans. ASM*, 1969, vol. 62, p. 155.
33. P. M. Hazzeldine and D. E. Newbury: Proceedings of ICSMA3, Institute of Metals, London, England, 1973, vol. I, p. 202.
34. R. L. Coble: *J. Appl. Phys.*, 1963, vol. 34, p. 1679.
35. J. Bardeen and C. Herring: in "Imperfections in Nearly Perfect Crystals," W. Shockley, ed., J. Wiley, New York, NY, 1952, p. 279.
36. W. Beere: *Scripta Metall.*, 1978, vol. 12, p. 337.
37. S. Floreen: *Scripta Metall.*, 1967, vol. 1, p. 19.
38. R. C. Gifkins: *J. Inst. Metals*, 1967, vol. 97, p. 373.
39. I. W. Hall, T. Livini, E. Ganin, and A. Rosen: *Strength of Metals and Alloys*, P. Hassen, *et al.*, eds., Pergamon Press, 1979, vol. 1, p. 451.
40. S.-A. Shei and T. G. Langdon: *Acta Metall.*, 1978, vol. 26, p. 639.
41. T. Kainuma, A. Arieli, and A. K. Mukherjee: unpublished research, University of California, Davis, CA, 1980.
42. T. Chandra, J. J. Jonas, and D. M. R. Taplin: *J. Mater. Sci.*, 1978, vol. 13, p. 2380.
43. R. B. Vastava and T. G. Langdon: *Acta Metall.*, 1979, vol. 27, p. 251.
44. P. Sharriat, T. G. Langdon, and R. B. Vastava: presented at 109th AIME Annual Meeting, Las Vegas, NV, 1980.
45. R. Z. Valiev and O. A. Kaybyshev: *Phys. Stat. Sol(a)*, 1977, vol. 44, p. 65.

46. R. C. Gifkins: *Trans. TMS-AIME*, 1959, vol. 215, p. 1015.
47. J. L. Walter and H. E. Cline: *Trans. TMS-AIME*, 1968, vol. 242, p. 1823.
48. F. A. Mohamed and T. G. Langdon: *Philos. Mag.*, 1975, vol. 32, p. 697.
49. F. A. Mohamed and T. G. Langdon: *Acta Metall.*, 1975, vol. 23, p. 117.
50. B. J. MacLean: M. S. Thesis, University of California, Davis, CA, 1980.
51. A. Arieli, unpublished research, University of California, Davis, CA, 1980.
52. J. Hedworth and M. J. Stowell: *J. Mater. Sci.*, 1971, vol. 6, p. 1061.
53. A. Arieli and A. Rosen: *Scripta Metall.*, 1976, vol. 10, p. 471.
54. A. Arieli and A. K. Mukherjee: *Scripta Metall.*, 1980, vol. 14, p. 891.
55. B. Burton: *Diffusional Creep in Polycrystalline Materials*, Trans. Technol. Publications, Bay Village, OH, 1977, p. 96.
56. C. I. Smith, B. Norgate, and N. Ridley: *Scripta Metall.*, 1974, vol. 8, p. 159.
57. A. Arieli and A. K. Mukherjee: *Scripta Metall.*, 1980, vol. 14, p. 891.
58. A. E. Geklini and C. R. Barrett: *J. Mater. Sci.*, 1976, vol. 11, p. 510.
59. P. H. Pumphrey: in "Grain Boundary Structure and Properties," G. A. Chadwick and D. A. Smith, eds., Academic Press, London, 1976, p. 139.
60. H. Gleiter and B. Chalmers: *Prog. Mater. Sci.*, 1972, vol. 16, p. 1.
61. A. Arieli and A. K. Mukherjee: *Scripta Metall.*, 1979, vol. 13, p. 331.
62. S.-A. Shei and T. G. Langdon: *Acta Metall.*, 1978, vol. 26, p. 1153.
63. F. A. Mohamed, S.-A. Shei, and T. G. Langdon: *Acta Metall.*, 1975, vol. 23, p. 1443.
64. G. Herriot, B. Baudelet, and J. J. Jonas: *Acta Metall.*, 1976, vol. 24, p. 687.
65. D. L. Holt and W. A. Backofen: *Trans. ASM*, 1966, vol. 59, p. 755.
66. M. A. Gjostein: in "Diffusion," ASM, Metals Park, OH, 1973, p. 241.
67. D. Bergner and W. Lange: cited in Ref. 60.
68. Y. Adda and J. Philibert: *La Diffusion Dans Les Solides*, Presses Universitaires De France, Paris, 1966, p. 1148.
69. D. Juve-Duc, D. Treheux, and P. Guirlandeng: *Scripta Metall.*, 1978, vol. 12, p. 1107.
70. R. Rosenberg: *J. Vac. Sci. Technol.*, 1972, vol. 9, p. 263.
71. P. R. Howell, A. R. Jones, and B. Ralph: *J. Mater. Sci.*, 1975, vol. 10, p. 1351.
72. D. Delannay, A. M. Huntz, and P. Lacombe: *Scripta Metall.*, 1979, vol. 13, p. 419.
73. J. Bernardini and G. Martin: *Scripta Metall.*, 1976, vol. 10, p. 833.
74. A. N. Stroch: *Philos. Mag.*, 1955, vol. 46, p. 968.
75. D. M. Avery and W. A. Backofen: *Trans. ASM*, 1965, vol. 58, p. 551.
76. R. C. Cook and N. R. Rosebrough: *Scripta Metall.*, 1968, vol. 2, p. 487.
77. K. T. Aust and B. Chalmers: *Metall. Trans.*, 1970, vol. 1, p. 1095.
78. *Grain Boundary Structure and Properties*, G. A. Chadwick and D. A. Smith, eds., Academic Press, London, 1976, p. 201.
79. E. Venkatesh and L. E. Murr: *Scripta Metall.*, 1976, vol. 10, p. 477.
80. L. E. Murr: *Metall. Trans. A*, 1975, vol. 6A, p. 505.
81. K. Tangri and T. Malis: *Surface Sci.*, 1972, vol. 31, p. 101.
82. R. A. Varin and K. Tangri: *Scripta Metall.*, 1980, vol. 14, p. 337.
83. D. Grivas: Ph.D Dissertation, University of California, Berkeley, CA, 1978.
84. G. R. Kegg, C. A. P. Horton, and I. M. Silcock: *Philos. Mag.*, 1973, vol. 27, p. 1041.
85. G. Gurewitz: work in progress, University of California, Davis, CA.